THE POLARIZATION OF RADIO SOURCES

I. OBSERVATIONS OF SMALL DIAMETER SOURCES

By F. F. GARDNER* and R. D. DAVIES†

Summary

This paper is concerned with the observations of the polarization of small diameter radio sources made in 1963 with the Parkes 210 ft telescope over the wavelength range 11–74 cm. The sources of error in making such measurements with a single dish are discussed. At the short-wave end, the main limitation is system noise, and there is some complication from a slight variation of antenna gain with polarization angle; at long wavelengths, the limitation is the fine-scale structure of the galactic polarization in the direction of the source. The latter varies greatly across the sky.

A total of 164 sources were measured for polarization at 11·3 and 21·5 cm. Of the stronger sources, 90 were measured at 31 cm, 37 at 48 cm, and 18 at 74 cm. The general tendency was for the degree of polarization to decrease with increasing wavelength, and only three sources were found to have more than 2% polarization at 74 cm. For the sources with detectable polarization at 48 and 74 cm, the polarization at these wavelengths was often greater than expected from the short-wave measurements on the basis of a simple model of depolarization by Faraday rotation within the source.

I. INTRODUCTION

The intensity and spectrum of non-thermal radiation at radio wavelengths have been satisfactorily explained as originating in synchrotron emission from relativistic electrons spiralling around magnetic lines of force. The theory also predicts that the radiation should be substantially (over 70%) linearly polarized. The failure to detect this polarization in early measurements of radio sources at metre wavelengths could be understood if the magnetic field directions varied widely in the sources or if the radiation was depolarized by Faraday rotation effects.

The first detection of linear polarization in an extragalactic radio source was reported by Mayer, McCullough, and Sloanaker (1962). At 3 cm wavelength, the polarization of Cygnus A was found to be 8%, whereas at 9·5 cm it was less than 1%. Early observations made with the Parkes 210 ft telescope and a sensitive receiving system at 20 cm wavelength (Gardner and Whiteoak 1962) showed, surprisingly, that this very rapid depolarization at longer wavelengths was not typical of radio sources, and that in fact an appreciable fraction of extragalactic radio sources were polarized at 20 cm, with values up to 8% for unresolved sources and up to 40% in certain areas in resolved sources.

* Division of Radiophysics, CSIRO, University Grounds, Chippendale, N.S.W.
† On leave from Nuffield Radio Astronomy Laboratories, Jodrell Bank, England.

The general tendency for the degree of polarization to decrease with increasing wavelength was confirmed in measurements at Parkes in the 10–30 cm range (Gardner and Whiteoak 1963) and in interferometric observations at California Institute of Technology (Morris and Berge 1964). However, the depolarization varied markedly from source to source both in the average rate of decrease with wavelength and also in the general way in which the change took place. The phenomenon was evidently more complicated than envisaged in the simple models of source depolarization by Faraday rotation, such as had been proposed by Woltjer (1962).

TABLE 1

PARTICULARS OF RECEIVING SYSTEMS

Centre Frequency (Mc/s)	Wavelength (cm)	I.F. Bandwidth (Mc/s)	$\mathscr{R}_1$ (rad/m²)	Overall Noise Temperature (°K)	Feed System	Beamwidth
2650	11·3	50	4000	180	Rectangular horn	7'·5 by 7'·2
1410	21	10	3500	100	Double-dipole† unit	14'·2 by 14'·0
960	31	8*	430	400	Rectangular horn	19'
630	48	8*	110	350	Double-dipole†	31'
404	74	8*	30	300	Double-dipole†	48'

* Double-sideband receivers with two channels 8 Mc/s wide, centres separated by 20 Mc/s.
† Two dipoles 0·4λ apart and 0·25λ above a reflecting plate.

The early observations of Gardner and Whiteoak (1963) indicated a correlation between depolarization and surface brightness of the sources, with a possible dependence upon galactic latitude. It was evident that results were required for a larger sample of sources to test such dependences, while, to check the mechanism of depolarization, as wide a wavelength range as possible should be covered. The observations to be described in the present paper (Part I of a series), made up to the end of 1963, were undertaken in an attempt to fill this need. The paper is concerned primarily with the observations of the smaller diameter radio sources, but results for a number of extended sources are included in the tabulation. Values are given separately for the components where they are 7' arc or more apart and clearly resolved by the 11 cm beam; central values only are given for sources partially resolved. The detailed treatment of extended sources will be covered in Part II of the series, while the discussion of the polarization results and their correlation with source parameters and the properties of the intervening ionized medium will be given in Part III. The Faraday rotation for the polarized sources of the present paper has been described in an earlier paper (Gardner and Davies 1966). The 20 cm polarization data for sources in the declination range −20° to −60° were discussed by Bolton, Gardner, and Mackey (1964).

II. OBSERVATIONAL PROGRAM

The bulk of the observations were made between March and November 1963. At 11 and 20 cm, 164 sources were measured; of these, 90 were measured at 30 cm, 37 at 50 cm, and 18 at 75 cm. Receiving systems with low-noise parametric amplifiers

and Dicke switching were used at 11 cm (Cooper, Cousins, and Gruner 1964) and at 20 cm (Gardner and Milne 1963). The observations at the longer wavelengths were made with double-sideband mixer receivers operated as total power radiometers. Relevant details of receivers and feed systems are given in Table 1. The quantity $\mathscr{R}_1$ of Table 1 will be discussed in Section III.

Rotary joints and low-loss lines from feed to receiver were used at 11 and 20 cm. Flexible RG-9 cables were used at the other wavelengths. The linearly polarized feeds were mounted in a reflecting plate about 6 ft in diameter. In observations before November 1963, only the central 19 in. of the plate rotated, but in later observations the whole plate turned. A full rotation occupied 2 min of time.

(a)   AFTER TRANSIT   (b)   BEFORE TRANSIT
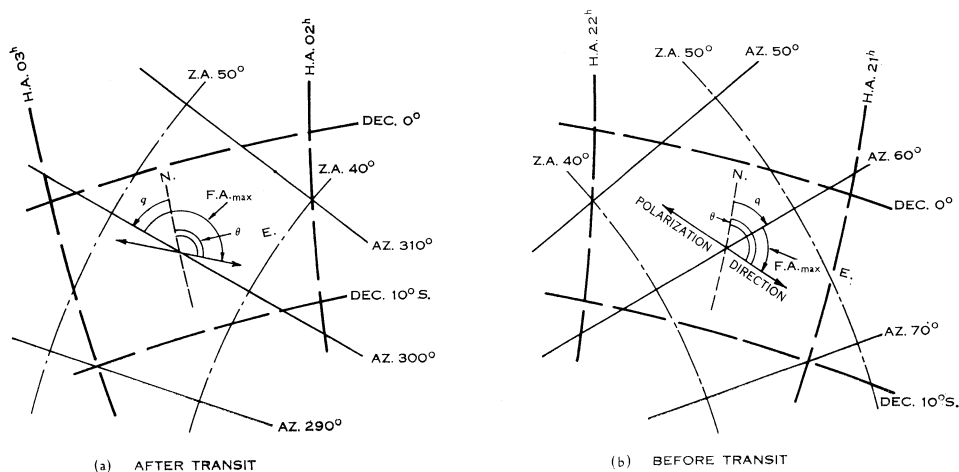
Fig. 1.—Illustration of the angles involved in the measurement of polarization with the Parkes telescope, which has an altazimuth mount. The same source at declination 5° S. is shown $2\frac{1}{2}$ hr before and $2\frac{1}{2}$ hr after transit. The angle labelled F.A.$_{max}$ is the angle, measured from the vertical circle through the Parkes zenith (latitude 33° S.) and the source, at which the intensity is a maximum. The parallactic angle q, which is added to F.A.$_{max}$ to give the position angle of polarization, is positive before and negative after transit. At feed angle zero, the electric vector is vertical.

III. MEASUREMENT OF POLARIZATION

The basic observation consisted of the measurement of source intensity as a function of the angle of the linearly polarized feed system at the focus of the 210 ft telescope. The polarization angle of the feed could be measured to an accuracy of better than $\frac{1}{2}°$, but it was not possible to check directly that the polarization of the incoming radiation was unchanged by reflection at the dish surface. It is considered that such deviations probably do not exceed 1° at the wavelengths used. A measurement to this accuracy will be made in checking the instrumental effects in polarization interferometry. At present we can only conclude from the internal consistency of measurement of the more intense highly polarized sources, made at varying hour angles, that the deviations are certainly less than 3°.

In most of the observations, the receiver output was measured as the feed system rotated,* with the telescope tracking firstly the source (the "on-source" variation) and then the "off-source" comparison region. The "off-source" was subtracted from the "on-source", and a sine wave with an angular period of 180° was fitted to this difference. The degree of polarization is given by the ratio of the amplitude of this sine wave to the mean intensity and is usually expressed as a percentage. Because of the altazimuth telescope mount, the parallactic angle (positive before transit) has to be added to the feed angle of maximum electric field to give the position angle measured east of north. The situation is illustrated in Figure 1 for a polarized source (position angle 110°) at declination −5°, measured with the Parkes (latitude 33° S.) telescope $2\frac{1}{2}$ hr before and then $2\frac{1}{2}$ hr after transit.
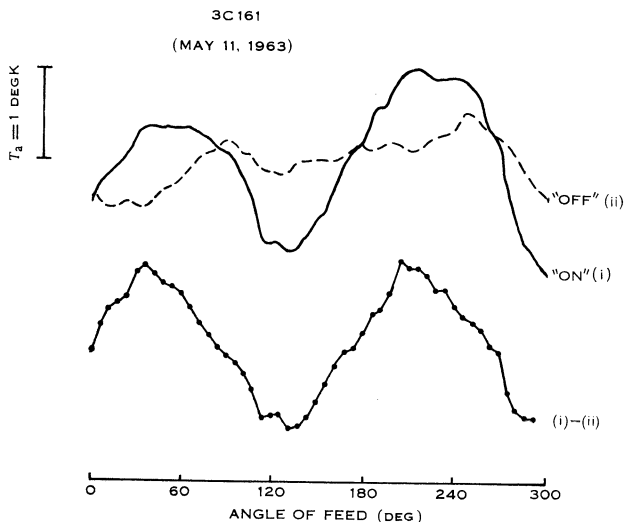

Fig. 2.—"On-source" (i) and "off-source" (ii) variations of receiver output with the rotation of the feed system. The source is 3C 161 and the frequency 2650 Mc/s. The sine wave component with a period of 180° in the difference (i) − (ii) is the source polarization. (For convenience, the mean level of (ii) has been adjusted to coincide approximately with (i).)

We have

$$\text{position angle of polarization} = \text{feed angle of maximum intensity} + \text{parallactic angle}$$

or, symbolically, $\theta = \text{F.A.} + q.$

A typical record is shown in Figure 2. The "off-source" variation at the shorter wavelengths is considered to be due mainly to the variation of the amount of ground radiation picked up by the dish spillover lobes as the feed system rotates. Since the

---

*The alternative method, measuring source intensities for a sequence of six polarization angles 0°, 30°, . . . , 150°, was sometimes used. However, it was found that for the same overall observing time the accuracy of the polarization measurement was considerably lower than with the continuous rotation method.

intensity variation during rotation usually considerably exceeds the polarization being measured, it is necessary to ensure that it is the same in the two instances. Hence, the "off-source" comparison region was generally chosen to be at the same declination as the source, and the rotation of the feed was started at the same hour angle "on" and "off" source. In most of the observations, this meant a difference of $\pm 4^m$ in right ascension of the two positions. This was made up of $3\frac{1}{2}$ min for the rotation from $0°$ to $300°$ and back to $0°$, plus $\frac{1}{2}$ min for the telescope drive to the second position.

The effect of the receiver time constant is to reduce the apparent degree of polarization and to change the angle of maximum intensity, the sign of the angular change depending on the sense of rotation. Corrections of $0·5\%$ or 2% and $3°$ or $6°$, appropriate to time constants of 1 or 2 sec, were applied.

Because of Faraday rotation, the polarization angle θ (rad) varies with the wavelength λ (m); thus (Gardner and Whiteoak 1963),

$$\theta = \theta_0 + \mathscr{R}\lambda^2,$$

where θ_0 is the intrinsic polarization angle at $\lambda = 0$, and $\mathscr{R}$ is the rotation measure. In general then, the polarization angle will vary across the receiver pass band, and the amount of this change will increase with $\mathscr{R}$. As $\mathscr{R}$ increases, the effect is to decrease the apparent degree and not the angle of polarization (see Appendix), with the polarization first falling to zero for a rotation measure of $\mathscr{R}_1$. The $\mathscr{R}_1$ value appropriate to each wavelength is given in Table 1. The only source with definite polarization where $\mathscr{R}$ exceeds $\mathscr{R}_1$ is Pictor A at 75 cm. For $\mathscr{R}$ greater than $\mathscr{R}_1$, the angle observed would be in error by $90°$ (see Appendix) if the two pass bands were accepted equally. No corrections for bandwidth effects have been applied in the source list.

IV. Spurious Polarization Effects

(a) Instrumental Effects

There are three main instrumental effects that can give rise to spurious polarization:

(i) *beam "ellipticity" effect*, which arises when the beam is elliptical in cross section and the axis of this ellipse rotates with the feed system;

(ii) *beam "squint" effect*, which is caused by a variation of the beam-pointing with the angle of the feed;

(iii) *variation of telescope aerial gain* with rotation.

It has been found that (i) and (ii) are negligible when measurements are made of small diameter sources and the pointing error is not more than $1'·5$. Their evaluation and the application of corrections will be discussed in detail in Part II (extended sources).

Aerial gain variation (iii) has been found significant only at 11 cm, the shortest wavelength used in these observations. Sources of low expected polarization, including the HII regions Orion A, M17, Sagittarius A, and 30 Doradus, were all found to have maximum intensity near zero feed angle, irrespective of the parallactic angle. There

was some evidence that the degree of polarization varied slightly with the angular size of these sources and with zenith angle, but almost all the observed values for the above sources were within the range of apparent polarization $1 \cdot 3 \pm 0 \cdot 3 \%$ and of feed angle $0° \pm 10°$. Since there is no change with parallactic angle (see Fig. 1), it is clear that this is an instrumental polarization, and so a correction must be applied to the values measured for the remainder of the sources. This consisted of subtracting* a vector of length $1 \cdot 3 \%$ at F.A. $= 0°$ from the vector representing the measured percentage polarization and feed angle. The subtraction was made before the parallactic angle was added.

At 20 cm the gain variation was less than $0 \cdot 3 \%$, and no correction was necessary.

(b) Galactic Polarization Effects

Normally, the polarization at the source position S was measured with respect to that at a comparison point C_{+4}, 4^m higher in right ascension, and then with respect to C_{-4}, 4^m lower. At 11 cm, with one or two exceptions, the two values $S—C_{+4}$ and $S—C_{-4}$ agreed within the limits set by noise fluctuation. At 20 cm, there were measurable differences in about half the cases, that is, C_{+4} and C_{-4} were different. At longer wavelengths, the differences were generally found to be greater.

From the following argument, it was inferred that $C_{+4}—C_{-4}$ is the difference in the polarized galactic emission between the two points 8^m apart in right ascension.

(1) The main beam was sufficiently circular in each case for beam "ellipticity" effects operating on gradients in the background emission to be negligible.

(2) As described previously, each pair of points compared were observed with the same telescope azimuth and zenith angles, and so ground radiation and receiver effects are removed in the differences.

(3) Observations repeated at different hour angles gave the same intensity and position angle for $C_{+4}—C_{-4}$, indicating that the polarization being measured originates in the main beam and not in distant side lobes; this is supported by the fact that fine structure comparable with the beamwidth is sometimes found.

(4) The average wavelength dependence of $C_{+4}—C_{-4}$, between λ^2 and λ^3 in brightness temperature units, was similar to the spectrum of the galactic background, the polarization of which has been established at 75 cm.

If the background polarization varied uniformly across the source, then the average of the two values $S—C_{+4}$ and $S—C_{-4}$ would give the source polarization without error. From observations over a range of positions in the vicinity of a number of sources, to be described below, it appeared that errors caused by departures from a uniform gradient should not exceed $\frac{1}{2}(C_{+4}—C_{-4})$, or half the difference between the nearest pair of points, in more than 10% of the cases. These error values have been used in the source list and combined with the signal-to-noise errors as independent errors. In addition to this increase in error, the true source polarization will be

* The fact that the angular period is $180°$ must be remembered in making the vector subtraction. Thus, a measured polarization value of $2 \cdot 2 \%$ at feed angle $45°$ becomes, after correction, $2 \cdot 6 \%$ at feed angle $60°$.

lower on the average than the measured value, which is the vector sum of the polarization of the source and of the background in the source direction. In the extreme case of an unpolarized source, the measured value is just that of the background. The reduction will be important when the two contributions are approximately equal, and we might estimate roughly that the true source polarization would then lie about midway between the measured value and the lower limit set by the galactic background (this is illustrated later in Figure 4; the effect is marked in the case of 3C 279 at 75 cm).

Figure 3 shows polarization vector plots, with a 2θ position angle scale, for some pronounced cases of background polarization. For source 1424−41 at 20 cm, the point S could well fit the sequence C_{-4}, C_{-2}, etc. and the source polarization be zero. Background effects were significant for this source even at 11 cm. Hercules A has definite polarization at 20 cm (Fig. 3(b)). The polarization measured with respect to points $\pm 2^{m}$ is not greatly different from the value for the usual $\pm 4^{m}$. Source 16−01 (Figs. 3(c) and 3(d)) is polarized at 20 cm, but at 30 cm the source polarization is swamped by the background. $S-C_{+4}$ is nine times higher than $S-C_{-4}$.

Figure 3(e) shows a similar plot for the source 3C 273 at 74 cm, the longest wavelength at which measurements were made. The comparison points follow a smooth curve, and the source is polarized $2 \cdot 4 \pm 0 \cdot 7\%$, a value almost as high as at 11 cm.

It is apparent that the confusion from the background polarization can be reduced by using nearer comparison points, in both right ascension and declination. However, there is a limit, since, at about $1 \cdot 2$ beamwidths from the source, spurious "ellipticity" and "squint" effects begin to become significant. Interferometry is probably superior to single dish operation at wavelengths longer than 30 cm.

The measurement of the galactic background polarization in the immediate vicinity of each source, and the determination of its Faraday rotation, is important in its own right to establish a relative distance scale for the rotation for the source and for the background (Gardner 1964) and to check on possible reversals of magnetic field along the line of sight to the extragalactic source.

V. RESULTS

The measured values of polarization are given in Table 2. 3C and MSH numbers are given in addition to the Parkes catalogue numbers based on coordinates (Bolton, Gardner, and Mackey 1964). The positions given are accurate to 1′ arc. The errors in percentage polarization are obtained by combining the galactic background errors and those from sensitivity. The latter are given separately in parentheses. Thus, a source polarized $2 \cdot 8\%$ with a noise error of $0 \cdot 4\%$ and a background error $\frac{1}{2}(C_{+4}-C_{-4})$ of $0 \cdot 6\%$ is given as $2 \cdot 8 \pm 0 \cdot 7(0 \cdot 4)$. If no information were available about the background, it would be given as $2 \cdot 8 \pm -(0 \cdot 4)$. The position angle errors quoted are determined solely by sensitivity. Two entries are given for a number of double sources, such as 0131−36 and 0634−20, which are resolved by the $7' \cdot 4$ beam at 11 cm. At longer wavelengths these are not resolved, and the two values given are not independent. Their significance will be discussed in Part II of this series.

TABLE 2.

Source	Other Designations	Position (1950)		Galactic Coordinates		P (11.3)		P (21.5)	
		R.A. h m s	Dec. ° ′	l^{II} °	b^{II} °	%	p.a.	%	p.a.
0008−42		00 08 19	−42 09	329.7	−73.1	0.6±0.6	89±40	0.2±0.3(0.2)	89±15
0023−26	00−210	00 23 15	−26 19	42.2	−84.2	0.3±0.4	130±40	1.8±1.1(0.7)	110±10
0035−02	3C 17	00 35 44	−02 24	115.2	−64.8	1.3±0.3	2±8	0.5±0.7(0.5)	4±30
0038+09	3C 18	00 38 15	09 47	118.6	−52.7	1.8±0.7	108±18	3.0±2.1(1.1)	113±10
0043−42	00−411	00 43 55	−42 24	306.6	−75.0	10.1±0.7	139±3	9.8±—(0.6)	137±2
0045−25	00−222, NGC 253	00 45 05	−25 34	97.4	−88.0	<0.7		<0.7	
0053−01	3C 29(a)	00 53 39	−01 35	125.7	−64.2	2.8±2	22±20	1.7±3 (0.6)	176±15
0054−01	3C 29(b)	00 54 59	−01 39	126.4	−64.2	10.8±0.7	159±2	9.7±2.0(0.6)	161±2
0105−16	3C 32	01 05 48	−16 21	143.3	−78.3	2.8±1.2	60±20	0.9±—(0.6)	170±20
0106+13	3C 33	01 06 11	13 04	129.4	−49.3	7.3±0.3	81±2	8.2±—(0.3)	58±3
0114−21	01−26	01 14 23	−21 08	167.0	−81.5	<1.0		0.7±0.7(0.4)	70±10
0117−15	3C 38	01 17 58	−15 35	154.1	−76.4	2.0±0.7	112±7	0.5±—(0.9)	115±50
0123−01(a)	3C 40(a)	01 23 27	−01 38	142.2	−62.9	0.5±0.5	105±30	3.3±0 8(0.5)*	2±4
0123−01(b)	3C 40(b)	01 23 29	−01 33	142.2	−62.9	<1.6		3.3±0 8(0.5)*	2±4
0131−36(a)	01−311(a)	01 31 16	−36 45	261.9	−77.1	19.0±2.0	108±3	10.0±1.0(0.5)	124±4
0131−36(b)	01−311(b)	01 31 56	−36 44	261.5	−77.0	4.2±1.8	174±20		
0157−31	01−315	01 57 53	−31 08	231.1	−74.5	3.9±0.7	72±7	2.6±1.4(0 7)	100±6
0213−13(a)	3C 62(a)	02 13 10	−13 13	181.4	−65.8	7.2±0.8	91±5	5.3±0.7(0.5)	124±4
0213−13(b)	3C 62(b)	02 13 22	−13 26	181.9	−65.9			13.0±3.0(2.4)	110±7
0235−19	02−110	02 35 21	−19 46	201.3	−64.5	7.9±0.6	174±4	4.2±0.7(0.5)	12±3
0240−00	3C 71, 02−014	02 40 03	00 07	171.7	−51.7	0.3±0.3	105±20	0.3±0.5(0.3)	6±30
0252−71	02−72	02 52 25	−71 16	290.0	−42.9	0.2±0.4	105±35	1.0±0.7(0.5)	148±15
0255+05	3C 75, 02+010	02 55 02	05 51	170.2	−44.9	2.1±0.6	29±5	0.2±0.6(0.2)	50±30
0305+03	3C 78, 03+03	03 05 49	03 55	174.8	−44.5	3.0±0.5	98±6	2.6±1.0(0.4)	124±10
0307+16	3C 79	03 07 12	16 55	164.1	−34.4	7.6±0.5	6±3	7.0±1.5(0.4)	158±3
0316+16	CTA 21	03 16 07	16 18	166.6	−33.6	2.2±0.8	51±12	0.3±0.3(0.3)	1±10
0319−37	Fornax A(a)	03 19 39	−37 19	240.1	−56.9	14.6±1.1	64±2	12.3±0.5(0.5)	61±3
0322−37	Fornax A(b)	03 22 09	−37 26	240.2	−56.4	7.2±0.7	110±3	10.2±1.0(1.0)	101±3
0331−01	3C 89, 03−03	03 31 40	−01 21	186.3	−43.2	1.5±0.7	67±20	0.2±0.8(0.5)	50±50
0349−14	03−19	03 49 18	−14 38	205.5	−46.3			1.2±1.2(0.5)	66±8
0349−27	03−212	03 49 43	−27 55	224.6	−50.2	0.5±0.5	44±30	3.3±0.9(0.7)	5±6
0356+10	3C 98	03 56 10	10 18	179.8	−31.0	6.7±0.8	96±3	6.0±—(0.6)	74±5
0409−75	04−71	04 09 54	−75 15	289.0	−36.1	0.1±0.4	—	<0.2	
0427−53	04−54	04 27 50	−53 56	262.4	−42.4	3.0±0.8	157±7	0.7±0.7(0.5)	12±20
0438−43	04−49	04 38 46	−43 39	248.4	−41.6	0.7±0.3	73±10	1.0±—(0.5)	103±10
0442−28	04−218	04 42 45	−28 15	228.5	−38.8	1.6±0.4	130±9	3.7±1.3(0.4)	102±3
0453−20	04−222	04 53 14	−20 39	220.3	−34.4	2.7±0.5	117±4		
0453−30(a)	04−314(a)	04 53 16	−30 11	231.6	−37.0	6.6±0.8	100±3	4.9±1.0(0.5)	91±5
0456−30(b)	04−314(b)	04 56 28	−30 11	231.8	−37.5	7.0±1.1	113±7	5.1±1.8(0.8)	136±5
0511+00	3C 135, 05+02	05 11 24	00 54	200.4	−21.1	3.8±0.9	120±12	1.4±2.1(0.5)	118±12
0518+16	3C 138	05 18 14	16 37	187.4	−11.3	8.8±0.6	168±4	7.9±1.1(0.3)	168±3
0518−45	Pictor A	05 18 20	−45 49	251.6	−34.6	2.9±0.3	132±3	3.1±0.4(0.4)	50±5
0521−36	05−36	05 21 13	−36 32	240.6	−32.7	3.8±0.3	76±3	3.0±0.6(0.5)	89±4

*Components (a) and (b) unresolved at 21.5 cm.

POLARIZATION VALUES

P (29.7)		P (31.3)		P (48.3)		P (74.3)	
%	p.a.	%	p.a.	%	p.a.	%	p.a.
		1.2±1.3(0.6)	116±11				
		8.1± — (0.5)	146±5	6.4±1.2(0.6)	171±2	1.6±1.8(1.0)	93±30
		2.5±2.5(0.8)	65±10				
11.2±1.5	169±5	8.2±1.7(1.3)	178±4	4.2±2.5(0.6)	105±6	1.0±1.0(0.7)	136±12
		7.2±0.8(0.5)	24±6	3.6±1.1(0.4)	112±5	3.8±1.6(0.5)	164±12
		8.1±0.8(0.7)	134±7	7.0±2.0(0.9)	13±5	7.5±2.2(1.2)	97±6
<1.5		1.2±2.3(0.9)	12±20				
		5.2±1.6(0.7)	103±4				
		1.5±1.1(1.0)	38±15				
		4.8±1.4(1.0)	129±6	3.4±1.5(0.7)	167±10		
				2.2±11 (0.7)	42±10	2.3±6.1(1.4)	15±15
		9.3± — (0.5)	52±3	2.9±0.2(0.2)	25±2	0.5±0.25(0.2)	101±10
		8.9± — (0.3)	94±3	2.8±0.2(0.2)	56±4	0.9±0.25(0.2)	108±10
		1.1±0.8(0.4)	53±8				
		4.2± — (0.6)	112±6	<0.4			
		0.4±0.6(0.2)	18±15				
		0.8±0.5(0.4)	161±8				
		2.9±0.6(0.5)	1±4				
		<1.5					
		3.5± — (1.5)	70±15	4.0±2 (1.2)	69±6		
		7.7± — (1.5)	140±10	10.6±4 (2.0)	30±6		
		4.3± — (0.3)	141±5				
		2.8±0.5(0.5)	169±5	2.3±0.3(0.2)	157±3	0.7±0.2(0.2)	26±5
3.0± — (0.3)	111±9	2.2±0.8(0.3)	130±6	1.9±0.5(0.3)	43±6	1.5±0.3(0.2)	78±5

TABLE 2

Source	Other Designations	Position (1950)		Galactic Coordinates		P (11.3)		P (21.5)	
		R.A. h m s	Dec. ° ′	l^{II} °	b^{II} °	%	p.a.	%	p.a.
0531+22	Taurus A, 3C 144	05 31 26	22 00	184.5	−05.8	3.8±0.5	132±5	1.6±0.1(0.1)	86±2
0532−05	Orion A, 3C 145	05 32 47	−05 25	209.0	−19.4	0.1±0.4	—	0.3±—(0.2)	104±20
0539−69	30 Doradus	05 39 08	−69 07	279.5	−31.7	0.1±0.4	—	0.1±0.1(0.1)	70±25
0602−31		06 02 20	−31 56	238.2	−23.3	2.3±0.9	72±7	0.6±0.8(0.4)	29±15
0604−20	06−22	06 04 24	−20 22	226.8	−18.7	1.4±1.0	83±17	0.9±1.2(0.8)	31±25
0614−34		06 14 50	−34 55	242.1	−21.8	1.1±0.6	100±12	2.1±1.7(0.8)	85±10
0618−37		06 18 13	−37 10	244.7	−21.9	8.7±0.7	67±3	14.0±4.3(2.0)	71±6
0620−52	06−53	06 20 36	−52 40	261.1	−25.6	2.7±0.6	97±8	1.3±0.8(0.5)	30±12
0624−05	3C 161, 06−04	06 24 43	−05 51	215.4	−08.1	9.5±0.3	173±2	5.7±0.3(0.3)	23±3
0625−53	06−55	06 25 18	−53 39	262.4	−25.1	2.7±0.5	134±4	0.4±0.9(0.5)	55±35
0625−35	06−38	06 25 24	−35 28	243.5	−20.0	3.6±0.6	14±7	0.5±—(0.3)	8±15
0634−20(a)	06−210(a)	06 34 19	−20 30	229.9	−12.4	7.0±1.2	116±7	7.4±—(0.6)	0±4
0634−20(b)	06−210(b)	06 34 19	−20 37	230.0	−12.4	17.2±1.5	141±2	8.0±—(0.6)	43±4
0637−75	06−71	06 37 33	−75 13	286.4	−27.1	2.6±0.5	13±4	3.6±—(0.5)	58±4
0704−23	07−21	07 04 28	−23 07	253.3	−07.2	1.7±0.9	137±10	<1.1	
0715−24	07−24	07 15 14	−25 00	238.2	−05.9	3.1±0.5	111±4	4.0±—(0.7)	46±5
0719−55	07−53	07 19 13	−55 20	266.6	−18.2			0.7±—(0.6)	140±25
0750−26	07−215, NGC 2467	07 50 18	−26 18	243.2	00.4	0.7±0.3	27±15	0.6±0.4(0.2)	96±5
0806−10	3C 195	08 06 30	−10 19	231.4	12.0	2.3±1.4	72±12	1.0±0.6(0.4)	14±7
0813−35		08 13 54	−35 23	253.5	−00.3	2.6±1.2	38±20	<0.6	
0814−35(a)		08 14 14	−35 26	253.6	−00.2	0.6±0.9	102±40		
0814−35(b)		08 14 54	−35 26	253.7	−00.1	0.9±1.2	65±40		
0822−42	Puppis A	08 22 24	−42 50	260.6	−03.1	1.8±0.5	17±10	<0.4	
0842−75	08−71	08 42 18	−75 29	289.4	−19.9	5.7±1.1	160±8	1.0±—(0.7)	172±10
0855+14	3C 212	08 55 52	14 19	214.0	34.5			0.7±1.7(0.6)	71±6
0857−47	CTB 31	08 57 21	−47 20	267.9	−01.1	0.4±0.2	77±12		
0857−43	CTB 32	08 57 40	−43 34	265.1	01.5	0.3±0.3	80±25	0.2±0.1(0.1)	152±15
0859−25	08−219	08 59 37	−25 44	251.8	13.4	5.5±0.7	78±6	3.2±—(0.6)	23±6
0902−38	09−32	09 02 19	−38 32	262.0	05.4			1.9±—(1.2)	47±8
0915−11	Hydra A, 3C 218	09 15 40	−11 53	242.9	25.1	<0.3		0.1±0.1(0.1)	41±30
0945+07	3C 227, 09+07	09 45 04	07 39	228.6	42.3	5.4±0.8	152±9	5.5±—(0.4)	136±2
1005+07	3C 237, 10+01	10 05 22	07 45	232.1	46.6	0.5±0.7	43±45	<0.4	
1015−31	10−35	10 15 53	−31 29	268.6	20.7	<0.7		1.1±1.8(0.9)	38±22
1017−42	10S4A, 10−44	10 17 59	−42 36	275.6	11.8	3.4±0.7	77±7	2.9±—(0.5)	15±8
1142+19	3C 264	11 42 28	19 53	235.7	73.0	2.3±0.4	139±5	0.6±0.7(0.4)	3±14
1151−34	11−314	11 51 49	−34 49	289.9	26.3	0.8±0.6	176±30	2.4±2.0(0.5)	139±5
1215−45	12−43	12 15 26	−45 44	296.9	16.5	1.6±0.7	14±12	0.9±0.8(0.3)	153±6
1216+06	3C 270, 12+05	12 16 50	06 06	281.8	67.4	11.2±0.5	100±2	7.7±0.3	118±3
1222+13	M 84, 3C 272.1	12 22 31	13 10	278.2	74.5	5.7±0.4	145±3	2.4±0.9(0.4)	136±8

(*Continued*)

P (29.7)		P (31.3)		P (48.3)		P (74.3)	
%	p.a.	%	p.a.	%	p.a.	%	p.a.
		0.9±0.2(0.2)	10±4				
		2.8±1.8(1.0)	70±12				
		12.1±8.5(1.5)	64±4				
2.8±—(0.3)	49±5	2.0±0.6(0.5)	58±9	0.3±0.5(0.2)	33±30		
		0.9±—(0.5) <2.3	84±10				
4.1±—(1.0)	154±6	3.2±—(0.4)	8±5	} 7.6±0.7(0.5)	24±3	1.4±0.5(0.4)	179±8
				2 sources unresolved			
		4.0±—(1.0)	108±8	2.3±1.7(1.3)	104±15		
4.0±—(1.0)	119±8	2.1±14 (1.2)	14±15	<1.3		1.9±3.0(1.5)	15±30
		0.2±—(0.5)	—				
		2.7±—(1.5)	87±10				
		1.9±—(0.9)	102±10	3 sources unresolved			
0.2±0.2	126±25	0.5±—(0.3)	102±15				
		1.3±—(0.4)	13±6				
		5.6±—(2.0)	81±8				
		0.3±—(0.2)	63±8				
0.3±0.3(0.2)	83±20	1.7±—(0.7)	87±12				
<0.8		1.1±0.7(0.6)	80±6				
		0.5±0.5(0.4)	132±25	0.3±—(0.2)	136±25		
5.4±—(0.4)	126±3	4.9±—(0.4)	121±4	3.8±0.6(0.5)	42±3	1.8±1.0(0.6)	83±9
		<1.3					
		2.0±2.0(2.0)	160±30				
5.2±—(0.4)	139±6	5.5±0.4(0.3)	143±4	1.1±0.6(0.3)	62±6	1.6±1.3(0.3)	41±5
4.1±—(0.6)	46±8	3.8±—(1.2)	23±7				

TABLE 2

Source	Other Designations	Position (1950)		Galactic Coordinates		P (11.3)		P (21.5)	
		R.A. h m s	Dec. ° ′	l^{II} °	b^{II} °	%	p.a.	%	p.a.
1226+02	3C 273, 12+08	12 26 31	02 20	289.9	64.4	2.8±0.2	155±2	2.1±0.2(0.2)	155±2
1228+12	Virgo A, 3C 274	12 28 16	12 40	283.8	74.5	0.1±0.2	85±45	0.6±0.2(0.2)	147±8
1245−19		12 45 43	−19 43	301.9	42.9	0.6±0.4	99±15	1.3±1.2(0.5)	117±9
1246−41	12−45, NGC 4696	12 46 03	−41 02	302.4	21.6	0.7±0.8	101±35	<0.6	
1252−12	3C 278, 12−118	12 52 01	−12 17	304.1	50.3	6.1±0.2	2±3	5.1±—(0.5)	163±3
1253−05	3C 279, 12−020	12 53 33	−05 30	305.1	57.1	3.5±0.3	115±3	6.0±1.0(0.8)	153±8
1302−49	13−41	13 02 31	−49 12	305.3	13.3	0.1±0.5	—	<0.4	
1306−09	13−02	13 06 00	−09 34	309.9	52.8	0.8±0.6	159±25	0.7±0.8(0.6)	83±25
1308−22	13−23, 3C 283	13 08 55	−22 01	309.1	40.3	<1.0		1.0±0.7(0.5)	138±10
1322−42(a)	Cent. A(a)	13 22 04	−42 49	309.7	19.4	3.3±0.7	5±4		
1322−42(b)	Cent. A(b)	13 22 30	−42 44	309.5	19.4	16.8±0.5	95±2		
1323−61		13 23 03	−61 07	307.1	01.2	6.9±0.7	150±4	3.6±0.5(0.4)	119±5
1328+25	3C 287	13 28 14	25 25	22.5	81.0	3.4±0.4	110±3	0.5±0.5(0.2)	2±15
1332−33	13−33(a)	13 32 58	−33 38	313.4	28.1	7.3±1.0	93±3	3.7±1.0(1.0)	39±4
1333−33	13−33(b)	13 33 45	−33 43	313.5	28.0	20.8±1.0	103±2	12.2±1.0(1.0)	50±2
1334−33	13−33(c)	13 34 51	−33 54	313.7	27.7	24.0±1.5	94±2	19.9±1.0(1.0)	31±2
1334−29	NGC 5236	13 34 09	−29 37	314.6	32.0	1.0±0.8	130±25	0.6±2 (0.3)	61±15
1335−06	13−011	13 35 29	−06 12	323.2	54.6	4.8±0.8	167±6	1.0±0.8(0.5)	125±12
1343−60	13S6A	13 43 32	−60 08	309.7	01.7	2.3±0.3	40±4	1.5±0.5(0.5)	178±5
1355−41	13−45	13 55 57	−41 38	316.2	19.2	3.9±0.7	54±12	4.1±2.4(1.6)	13±7
1416+06	3C 298, 14+05	14 16 36	06 42	352.1	60.7	1.6±1.0	124±8	<0.7	
1424−41		14 24 47	−41 53	321.4	17.3	2.3±1.6	125±30	4.1±5.5(1.0)	105±5
1437−62	14−63	14 37 02	−62 27	315.1	−02.4			2.9±0.5(0.1)	154±4
1453−10	14−121	14 53 09	−10 56	345.3	41.3	1.3±1.0	62±20	1.3±1.4(0.6)	175±15
1459−41	14−415	14 59 01	−41 51	327.4	14.5	14.5±2.5	152±5	7.0±1.5(1.0)	142±5
1502+26	3C 310	15 02 48	26 12	38.5	60.2	2.7±0.3	38±6	<0.4	
1508−05	15−05	15 08 14	−05 32	353.9	42.9	2.7±0.6	58±4	3.1±0.7(0.5)	11±8
1514+07	3C 317, 15+05	15 14 16	07 12	09.4	50.1	1.0±1.0	110±30		
1526−42	15−43	15 26 51	−42 22	331.6	11.3	0.7±1.0	86±30	3.5±1.5(0.4)	101±4
1548−56	15−56	15 48 30	−56 03	326.8	−01.7	0.8±0.5	38±25	0.3±0.3(0.2)	87±15
1548−79		15 48 07	−79 31	310.8	−19.8	10.5±0.5	147±2	7.1±0.9(0.6)	43±3
1549−79		15 49 52	−79 05	311.2	−19.5	1.1±0.4	155±7	0.5±0.5	109±25
1559+02	3C 327(a), 16+01	15 59 56	02 06	12.5	37.8	5.1±0.3	163±3	6.0±—(0.9)	2±5
1602−09	16−01	16 02 45	−09 19	01.9	30.4	11.2±2	20±4	13.7±3 (1.5)	7±3
1610−60	16−61	16 10 45	−60 48	325.3	−07.2	3.3±0.4	86±4	0.5±0.3(0.2)	47±7
1611−77		16 11 14	−77 10	313.4	−18.9	<0.6		2.8±1.1(0.8)	163±5
1618−49		16 18 25	−49 58	333.6	−00.2	0.6±0.5	27±30	0.3±0.3(0.2)	118±10
1619−49	16−43	16 19 17	−49 27	334.1	00.1	<1.6		1.2±1.0(0.3)	59±5
1630−47	CTB 33	16 30 53	−47 29	336.8	00.0	1.0±0.5	61±12	0.6±—(0.2)	83±5
1636−46	16−47	16 36 02	−46 41	338.0	−00.0			0.2±—(0.1)	23±10
1637−77		16 37 27	−77 10	314.4	−20.0	2.0±1.0	150±15	2.0±0.7(0.5)	61±12

(*Continued*)

P (29.7)		P (31.3)		P (48.3)		P (74.3)	
%	p.a.	%	p.a.	%	p.a.	%	p.a.
$1.8\pm0.3(0.3)$	178 ± 10	$1.8\pm0.3(0.3)$	159 ± 4	$1.1\pm0.35(0.3)$	146 ± 6	$2.4\pm0.7(0.6)$	162 ± 6
		$0.5\pm-(0.2)$	167 ± 7				
		<3					
$7.8\pm0.8(0.7)$	14 ± 3	$6.4\pm0.7(0.6)$	12 ± 3	$4.9\pm2.5(1.3)$	122 ± 5	$3.3\pm2.5(1.5)$	15 ± 9
		$0.6\pm0.8(0.4)$	36 ± 20				
$1.6\pm-(0.6)$	40 ± 8	$1.7\pm1.3(0.5)$	44 ± 8	<0.5			
		$1.9\pm-(0.9)$	145 ± 20				
		$\}6.1\pm1.3(0.4)$	126 ± 2	$3.0\pm0.6(0.4)$	159 ± 5		
				2 sources unresolved			
$12.0\pm1.5(0.5)$	111 ± 2			$7.0\pm1.8(0.9)$	158 ± 5		
		$2.3\pm-(1.0)$	23 ± 10				
		$1.0\pm0.2(0.2)$	51 ± 4	$0.7\pm0.4(0.3)$	178 ± 10		
		$2.2\pm-(1.0)$	139 ± 12				
				$4.9\pm5.0(1.5)$	13 ± 8		
		$4.5\pm-(1.0)$	112 ± 15				
$1.7\pm-(0.6)$	78 ± 10	$1.5\pm-(0.7)$	113 ± 10				
$2.2\pm-(1.5)$	133 ± 10	$2.7\pm-(1.0)$	53 ± 15	$3.8\pm1.7(1.0)$	51 ± 10		
		$2.6\pm-(1.0)$	72 ± 10				
		$0.3\pm0.25(0.2)$	179 ± 15				
		$5.7\pm2.3(1.0)$	82 ± 5				
		$1.9\pm1.6(0.6)$	29 ± 12				
$3.3\pm-(0.7)$	55 ± 12	$3.0\pm0.9(0.8)$	34 ± 7				
		$14\pm11\ (1.1)$	128 ± 3				
		$0.4\pm0.4(0.2)$	72 ± 8				
		$1.7\pm\ -(1.0)$	34 ± 15				

TABLE 2

Source	Other Designations	Position (1950)		Galactic Coordinates		P (11.3)		P (21.5)	
		R.A. h m s	Dec. ° ′	l^{II} °	b^{II} °	%	p.a.	%	p.a.
1648+05	Herc. A, 3C 348	16 48 39	05 05	23.0	29.0	5.1±0.2	38±2	0.9±0.2(0.1)	41±2
1717+00	3C 353, 17−06	17 17 55	−00 57	22.9	20.6	6.6±0.2	114±2	2.9±0.3(0.2)	167±2
1727−21	17−211, 3C 358	17 27 43	−21 27	04.5	06.8	0.4±0.4	65±30		
1733−56		17 33 23	−56 32	335.4	−13.0	0.5±0.5	30±30	2.3±1.7(0.5)	175±6
1737−30	17−39	17 37 06	−30 57	357.7	−00.1	0.5±0.2	70±12	0.8±0.4(0.2)	61±5
1754−59	17−51	17 54 40	−59 47	333.8	−17.0	1.5±0.8	65±20	3.2±1.8(0.5)	77±5
1814−51	18−52	18 14 07	−51 59	342.3	−16.2	<1.0		2.6±2.1(0.5)	134±5
1814−63	18−61	18 14 52	−63 47	330.9	−20.8	0.6±0.5	131±20	0.2±0.6(0.2)	106±25
1817−16	M 17	18 17 36	−16 12	15.1	−00.7	0.4±0.3	170±30		
1821−12	18−18	18 21 13	−12 26	18.8	00.3	0.7±0.6	159±20	0.3± — (0.2)	128±20
1827−36		18 27 36	−36 05	358.3	−11.8	0.5±0.5	88±25	1.5±0.9(0.5)	25±8
1831−09	18−08(a)	18 31 09	−09 16	22.7	−00.3	1.7±0.3	170±5	0.5± — (0.2)	159±10
1831−08(a)	18−08(b)	18 31 33	−08 55	23.1	−00.3	1.8±0.5	173±8		
1831−08(b)	18−08(c)	18 31 34	−08 23	23.6	−00.0				
1846−00	3C 391, 18−012	18 46 49	−00 57	31.9	00.0	0.4±0.4	144±25	0.2±0.4(0.2)	14±30
1850+01		18 50 48	01 11	34.3	00.1	0.2±0.3	1±40		
1932−46	19−46	19 32 19	−46 27	352.2	−26.7	1.1±0.6	11±25		
1934−63		19 34 40	−63 49	332.7	−29.4	0.4±0.3	136±20		
1949+02	3C 403	19 49 44	02 23	42.3	−12.3	5.9±0.7	13±4	4.0±0.8(0.5)	124±5
1953−42	19−413	19 53 46	−42 31	357.5	−29.6	0.9±0.9	55±25	1.1±4.8(0.7)	117±20
1954−55	19−57	19 54 18	−55 17	342.8	−31.4	7.7±0.4	127±2	1.0±0.8(0.4)	92±12
2012+23	3C 409	20 12 17	23 26	63.4	−06.1	<0.5		0.6±0.7(0.7)	131±40
2032−35	20−37	20 32 39	−35 05	07.8	−35.6	7.0±1.0	90±4	8.0±0.8(0.5)	99±3
2045+06	3C 424, 20+010	20 45 43	06 50	53.7	−22.0	3.3±1.0	37±8	4.4±5 (0.5)	121±4
2058−28	20−215	20 58 38	−28 13	17.8	−39.6	1.7±0.7	67±8	2.8± — (0.6)	62±6
2104−25	21−21	21 04 23	−25 39	21.4	−40.2	2.2±0.5	36±7	2.2±0.7(0.4)	16±5
2121+24	3C 433	21 21 27	24 50	74.4	−17.7	6.3±0.4	108±2	5.2±0.5(0.5)	136±4
2140−43	21−47	21 40 25	−43 27	357.2	−49.0	4.4±1.5	94±5	4.7±2.3(0.5)	101±3
2150−52	21−58	21 50 49	−52 05	343.8	−48.8	<2		0.9±0.9(0.3)	112±7
2152−69	21−64	21 52 41	−69 56	321.3	−40.6	4.3±0.3	56±3	2.7±0.2(0.2)	116±4
2211−17	3C 444, 22−17	22 11 40	−17 16	40.2	−52.4	1.1±0.2	3±5	1.3± — (0.4)	178±5
2212+13	3C 442	22 12 15	13 36	75.1	−34.1	5.2±1.1	140±14	3.7±0.6(0.5)	53±4
2221−02	3C 445, 22−09	22 21 15	−02 22	61.9	−46.7	6.5±1.0	120±5	4.6±0.7(0.5)	132±3
2223−05	3C 446, 22−010	22 23 12	−05 15	58.9	−48.9	6.6±2.0	154±8		
2230+11	CTA 102	22 30 08	11 29	77.4	−38.6	5.0±0.4	16±3	6.6±1.7(0.5)	111±4
2250−41	22−46	22 50 14	−41 14	355.6	−62.0	4.1±0.7	74±5	2.1±0.9(0.4)	103±5
2314+03	23+05, 3C 459	23 14 02	03 48	83.0	−51.3	4.0±0.6	165±4	3.8±1.3(1.3)	
2331−41	23−44	23 31 48	−41 42	345.8	−68.7	1.3±0.6	10±25	0.7±0.6(0.4)	40±12
2335+26	3C 465	23 35 57	26 44	103.5	−33.1	3.7±0.5	84±4	0.2±0.2(0.2)	160±30
2356−61	23−64	23 56 24	−61 11	314.0	−55.1	4.5±0.5	24±4	4.9±0.3(0.3)	66±2

(*Continued*)

| P (29.7)		P (31.3)		P (48.3)		P (74.3)	
%	p.a.	%	p.a.	%	p.a.	%	p.a.
0.6± — (0.1)	15±3	0.7± — (0.2)	160±6	0.6±0.6(0.2)	1±8		
1.6± — (0.2)	101±2	<1.5	152±2	<0.2			
		1.0±0.8	136±25				
		0.9±0.9(0.7)	176±15				
		0.9± — (0.5)	95±15				
0.3± — (0.2)	37±20	<0.2					
		1.0±0.8(0.6)	32±15				
		1.0±1.3(0.5)	23±10				
		1.0±2.7(0.8)	138±25				
		2.0±1.5(0.5)	62±6				
		5.5±2.5(1.0)	19±3				
		3.9±1.9(0.5)	100±4	1.7±2.7(0.7)	124±15		
		1.0±0.5(0.3)	35±8	1.6±1.0(0.5)	66±10		
		7.4±2.4(0.6)	96±3	3.1±3.0(0.8)	99±10	3.8±4.7(1.2)	44±10
		1.3± — (0.5)	165±10	2.1±4.0(0.4)	22±8		
4.2± — (0.6)	155±8	3.6± — (0.5)	119±4	1.7±0.7(0.3)	87±8		
1.4± — (0.2)	166±5	1.1±0.3(0.2)	0±4			1.2±1.2(0.2)	24±4
		0.8± — (0.5)	39±7	0.4±1.0(0.4)	148±30		
		3.2±2.2(0.8)	115±4				
		3.2±0.8(0.5)	148±5	2.8±0.9(0.8)	138±10		
		3.1±0.2(0.2)	131±3	1.6±0.3(0.3)	166±4	0.9±0.45(0.2)	45±6
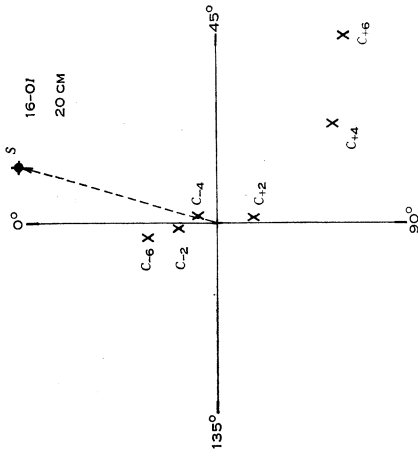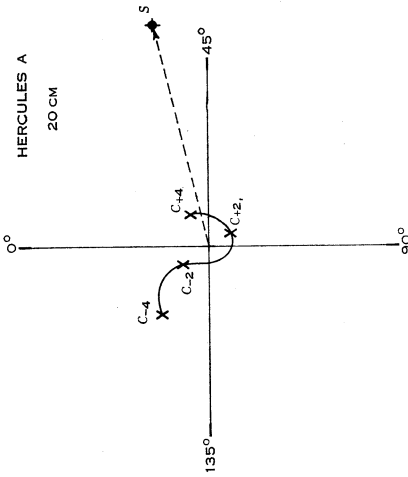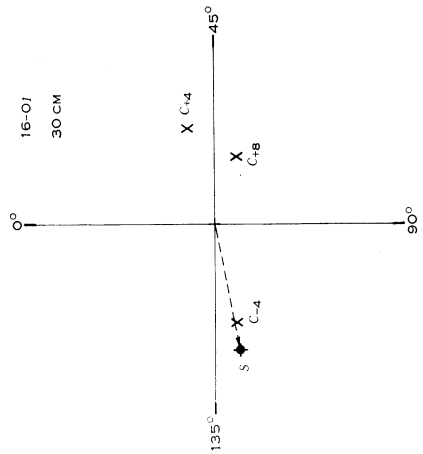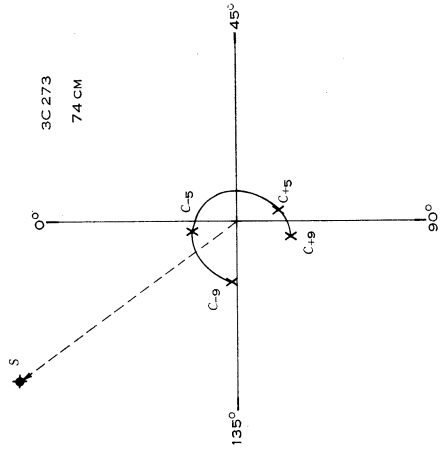
Fig. 3.—Polarization intensities and angles for sky positions in the vicinity of a number of radio sources. Point C_t gives the polarization at a point t min away in right ascension but at the same declination as the source, whose polarization is shown as S. The source number and wavelength of observation are shown in each case.

The general trend for the degree of polarization to decrease with increasing wavelength found previously (Gardner and Whiteoak 1963) is confirmed by the values of Table 2. However, a number of sources are still appreciably polarized at 50 cm and even at 75 cm, and plots of percentage polarization P against wavelength λ for some of these are given in Figure 4, which also includes, for comparison, three sources with more rapid depolarization, namely, Cygnus A (Hollinger, Mayer, and Mennella 1964), Hercules A, and $21-64$. In Figure 4, the smooth curves are drawn
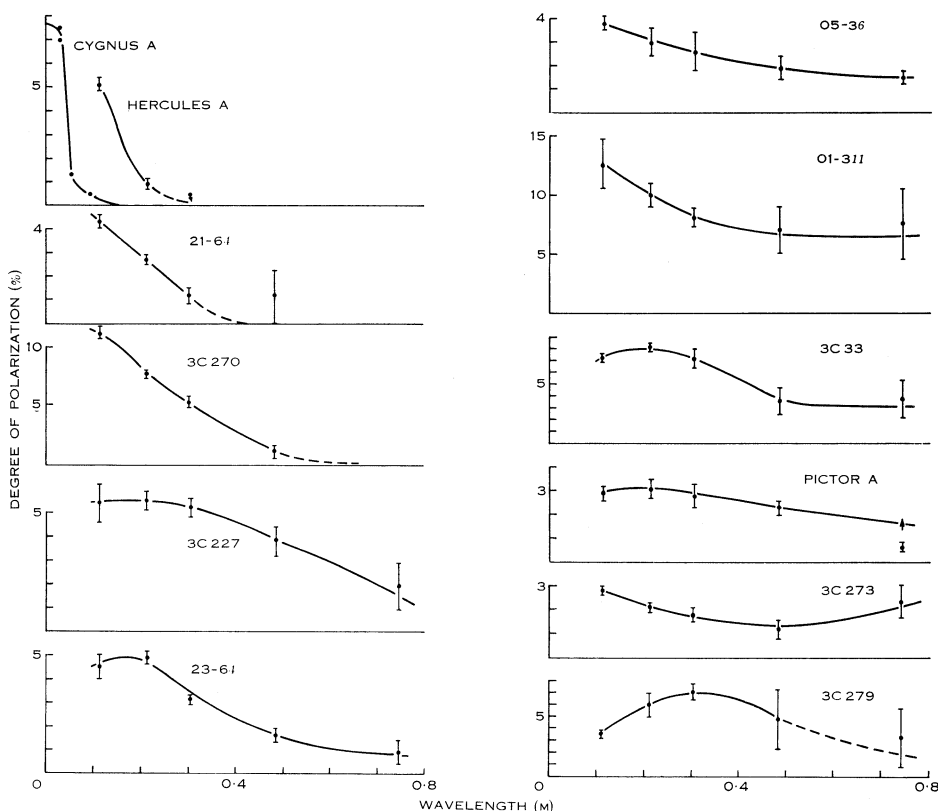

Fig. 4.—Degree of linear polarization versus wavelength for a number of sources. The 3C 279 value at $0 \cdot 75$ m is mainly galactic polarization (see text). Because of bandwidth depolarization, the true Pictor A value at $0 \cdot 75$ m is higher than observed. The source $01-311$ is resolved at 11 cm, the value used being a mean.

through intermediate values between the mean and the lower error limit when galactic polarization effects are appreciable (see Section IV(b)). They are continued dotted when the latter predominate. It should be remembered that the sources in Figure 4 are not typical (the general depolarization trend might lie between those shown for 3C 270 and $21-64$), and the sources measured at 50 and 75 cm were generally those with appreciable polarization at 30 cm and with rotation measures small enough for bandwidth effects to be small (see Table 1 and Appendix). Pictor A, mentioned earlier, is an exception, and its true polarization at 75 cm must

be considerably greater than the value shown, and its $P(\lambda)$ curve might be flat over the full wavelength range investigated.

The main feature of Figure 4 is the appreciable long wavelength extension to the $P(\lambda)$ curves, seen, for instance, in $01-311$, $05-36$, and 3C 33, an effect even more marked when P is plotted against λ^2, which is the relevant parameter if depolarization is by Faraday rotation effects.

The source 3C 279 is the best example of a reversal of the $P(\lambda)$ trend, the polarization at 11 cm being lower than at 20 and 30 cm. The reverse curvature of the spectrum (Bolton, Gardner, and Mackey 1964; Dent and Haddock 1965), with its minimum around 20 cm, suggests that 3C 279 has two components with different spectral indices. The polarization characteristics are consistent with the polarization occurring in only one component, namely, the one with the high spectral index which predominates at long wavelengths. This component might possess the usual $P(\lambda)$ trend, but the addition of unpolarized radiation from the second component at short wavelengths would reduce the overall degree of polarization. The measurements do not show any increase in polarized flux with increasing wavelength. A similar effect is probably present in 3C 273, the polarization residing in the jet with the steep spectrum, i.e. component A (Hazard, Mackey, and Shimmins 1962). The constancy of the polarization angle supports this interpretation (Gardner and Davies 1966).

A full discussion of the polarization characteristics and the interpretation of depolarization will be given in Part III of this series.

VI. Acknowledgments

VII. References

Bolton, J. G., Gardner, F. F., and Mackey, M. B. (1964).—*Aust. J. Phys.* **17**: 340.

Cooper, B. F. C., Cousins, T. E., and Gruner, L. (1964).—*Proc. Instn Radio Engrs Aust.* **25**: 221.

Dent, W. A., and Haddock, F. T. (1965).—*Nature* **205**: 487.

Gardner, F. F. (1964).—Symp. IAU–URSI No. 20 (Canberra 1963). p. 143.

Gardner, F. F., and Davies, R. D. (1966).—*Aust. J. Phys.* **19**: 129.

Gardner, F. F., and Milne, D. K. (1963).—*Proc. Instn Radio Engrs Aust.* **24**: 127.

Gardner, F. F., and Whiteoak, J. B. (1962).—*Phys. Rev. Lett.* **9**: 197.

Gardner, F. F., and Whiteoak, J. B. (1963).—*Nature* **197**: 1162.

Hazard, C., Mackey, M. B., and Shimmins, A. J. (1962).—*Nature* **197**: 1037.

Hollinger, J. P., Mayer, C. H., and Mennella, R. A. (1964).—*Astrophys. J.* **140**: 656.

Mayer, C. H., McCullough, T. P., and Sloanaker, R. M. (1962).—*Astrophys. J.* **135**: 656.

Morris, D., and Berge, G. L. (1964).—*Astr. J.* **69**: 641.

Woltjer, L. (1962).—*Astrophys. J.* **136**: 452.

APPENDIX

Effect of Bandwidth

For differential Faraday rotation, the change in angle $\Delta\theta$ across the receiving bandwidth Δf_1 is given by

$$\Delta\theta \doteq \frac{\mathrm{d}}{\mathrm{d}f}(\mathscr{R}\lambda^2)\,\Delta f_1$$

$$\doteq -\theta_0\frac{2\,\Delta f_1}{f_0} \qquad \text{with } \theta_0 = \mathscr{R}\,\lambda_0^2,$$

where $\mathscr{R}$ is the rotation measure, and λ_0 and f_0 are the central wavelength and frequency.

With a rectangular passband, the degree of polarization is reduced by a factor X below that for monochromatic radiation at wavelength λ_0. X is given by the usual diffraction grating* formula for a single slit

$$X = \sin\left(\frac{2\theta_0\,\Delta f_1}{f_0}\right)\Big/\left(\frac{2\theta_0\,\Delta f_1}{f_0}\right).$$

X has its first zero where $2\theta_0(\Delta f_1/f_0) = \pi$, or

$$\mathscr{R}_1 = \pi\left\{2\left(\frac{\Delta f_1}{f_0}\right)\lambda_0^2\right\}^{-1}.$$

For $\mathscr{R} = \frac{1}{2}\mathscr{R}_1$, $X = 2/\pi = 0\cdot64$.

With the double-sideband receivers, where the centres of the two bands are Δf_2 apart, the formula is equivalent to that for a two-slit diffraction grating, and

$$X = \cos\left(\frac{2\theta_0\,\Delta f_2}{f_0}\right)\sin\left(\frac{2\theta_0\,\Delta f_1}{f_0}\right)\Big/\left(\frac{2\theta_0\,\Delta f_1}{f_0}\right).$$

The first cosine factor is now more important, and X has its first zero when $2\theta_0(\Delta f_2/f_0) = \frac{1}{2}\pi$, or

$$\mathscr{R}_1 = \pi\left\{4\left(\frac{\Delta f_2}{f_0}\right)\lambda_0^2\right\}^{-1}.$$

For $\mathscr{R} = \frac{1}{2}\mathscr{R}_1$, X is now $0\cdot707$.

In each case, the polarization angle remains unchanged at the value appropriate to λ_0 until the first zero is reached. At this point, a difference of $\frac{1}{2}\pi$ appears, which continues until the following zero.

It should be emphasized that in practice the passbands are only approximately rectangular, and the two responses for the double-sideband receivers will differ slightly. The main effects of these will be near the zero points. The values of $\mathscr{R}_1$ for the different receivers used are given in Table 1.

---

* All angles are multiplied by 2 in the usual way for polarization to permit vector addition.